Mössbauer-effect studies and magnetization of grain-aligned $YBa_2(Cu_{1-x}Fe_x)_4O_8$: Debye-Waller-factor, electric-field-gradient, and critical-current anisotropies

P. Boolchand, S. Pradhan, Y. Wu, and M. Abdelgadir
Department of Electrical and Computer Engineering, University of Cincinnati, Cincinnati, Ohio 45221

W. Huff
Department of Geology, University of Cincinnati, Cincinnati, Ohio 45221

D. Farrell
Department of Physics, Case Western Reserve University, Cleveland, Ohio 44106

R. Coussement
Instituut Voor Kern En Stralingsfysika, 200D Celestijnenlaan, 3030 Heverlee, Belgium

D. McDaniel
Department of Chemistry, University of Cincinnati, Cincinnati, Ohio 45221
(Received 13 May 1991)

^{57}Fe Mössbauer-effect studies on grain-aligned $YBa_2(Cu_{1-x}Fe_x)_4O_8$ samples have permitted us to establish spatial anisotropy of the Fe Debye-Waller factor and electric-field-gradient parameters in the all-important CuO_2 planes. The ratio of the f factor parallel and perpendicular to the c axis, $f_c/f_{\perp c}=2.0(1)$. Our analysis shows V_{zz} to be positive and directed along the c axis but motionally averaged because of rapid fluctuations of oxygen atoms in the planes. Vibrating-sample-magnetometry measurements with the applied field parallel and perpendicular to the c axis show that the critical-current anisotropy $J_c/J_{\perp c}=3.25$ and is insensitive to Fe doping concentrations in the range $0\leq x\leq 0.03$.

I. INTRODUCTION

It is widely believed that superconductivity in the cuprates is largely confined to the two-dimensional CuO_2 planes, the structural element common to all cuprate superconductors. Spatial anisotropies in physical properties is a broad manifestation of the layered structure of these materials. Measurement of these anisotropies is critical to an understanding of these materials both from a basic science point of view as well as applications.

Fe as a dopant in $YBa_2Cu_4O_8$ (1:2:4) appears to replace Cu(2) sites in the planes exclusively, a point that we discussed in a recent publication.[1] This result is in sharp contrast to the same dopant largely replacing Cu(1) sites in the linear chains of the 1:2:3 phase.[2] Fe as a dopant in the 1:2:4 phase is thus of generic interest. Such doping studies provide, for example, a rather direct means to systematically alter the chemistry of the planes and to examine its effect on the structural, magnetic, and superconducting properties of these materials.

In this work, we report on room-temperature Mössbauer spectroscopy, x-ray diffraction, and T-dependent magnetization measurements on well-characterized $YBa_2(Cu_{1-x}Fe_x)_4O_8$ samples. Both polycrystalline and grain-aligned specimens were used. Grain alignment was achieved in an external magnetic field.[3] The grains align with the c axis colinear with the applied magnetic field. The use of the grain-aligned specimen in the Mössbauer experiments has permitted us, for the first time, to extract both the spatial anisotropy of the mean-square-displacement (MSD) tensor and the sign and orientation of the electric-field-gradient (EFG) tensor at Fe in the CuO_2 planes.

The results are surprising. These show that the MSD perpendicular to the c axis is a factor of 4 larger than the MSD along the c axis. This suggests that the dopant is localized away from the planes [in relation to Cu(2) sites] and towards the apical O(1) oxygen site. This displacement alone appears to be insufficient to account for the observed anisotropy. We suggest that anharmonicities in vibrational motion of Fe cation parallel to the planes must play a distinct role in contributing to this unusually large anisotropy. A specific proposal is advanced in this regard.

The observed quadrupolar doublet intensity asymmetry $[I_+/I_-(\beta)]$ as a function of the tilt angle ($=\beta$) between the c axis and the γ-ray propagation vector ($\mathbf{k}$) can be reconciled in terms of a positive electric field gradient with V_{zz} residing parallel to the c axis. However, we cannot account quantitatively for the measured $I_+/I_-(\beta)$ ratios assuming a purely static electric hyperfine interaction. Vibrational motion of the planar oxygen sites [O(3), O(2)] normal to the planes appears to produce a fluctuating EFG. At room temperature, the stationary relaxation process appears to be in the fast-relaxation regime. This motionally averages the radiation patterns of the quadrupole components to lower the observed I_+/I_- ratio from the expected theoretical value for the static case.

 ©1992 The American Physical Society

The use of grain-aligned 1:2:4 specimens in vibrating sample magnetometry experiments provides the critical current anisotropy $J_c/J_{\perp c}=3.25$ which is found to be insensitive to Fe doping at low concentrations ($x \lesssim 0.02$). We note that the critical-current anisotropy in the 1:2:4: phase is significantly smaller than the one (~ 10) in the homologous 1:2:3 phase.[3] Possible reasons for this result are discussed in relation to the crystal structure and known defects in these materials.

The paper is organized as follows. After describing the crystal structure of the Y-based 1:2:4 phase in Sec. II, we provide details on sample preparation and x-ray-diffraction (XRD) characterization of our samples in Sec. III. This is followed by experimental results on Mössbauer-effect and magnetization measurements in Sec. IV. A complete discussion of the Mössbauer spectroscopy results in relation to the Debye-Waller factors and the EFG tensor and magnetization results in relation to the critical-current anisotropies are presented in Sec. V. We conclude with Sec. VI, which provides a summary of the principal conclusions of this work.

II. CRYSTAL STRUCTURE OF $Y_1Ba_2Cu_4O_8$

The 1:2:4 phase crystallizes[4–6] in the *Ammm* space group with reflections indexed on an orthorhombic cell. The cell parameters at 300 K are $a=3.8413(3)$ Å, $b=3.8713(5)$ Å, $c=27.240(2)$ Å. The structure of 1:2:4 is closely related to that of 1:2:3, its homologous partner. Both cuprates possess two-dimensional CuO_2 planes with the 1:2:3 material possessing a linear (CuO_3) chain between a pair of (CuO_2) planes, but 1:2:4 possessing double chains (Cu_2O_4), i.e., ribbons between the pairs of (CuO_2) planes as sketched in Fig. 1. A remarkable feature of this structure is that the O(4) oxygen ribbon sites are three-fold coordinated instead of two as in the linear chains of the 1:2:3 material. This structural difference is thought to render the ribbons chemically more stable than the linear chains. This is probably the reason for the oxygen stability and the strikingly different Fe dopant site occupancy in the 1:2:4 material in relation to the 1:2:3 material.

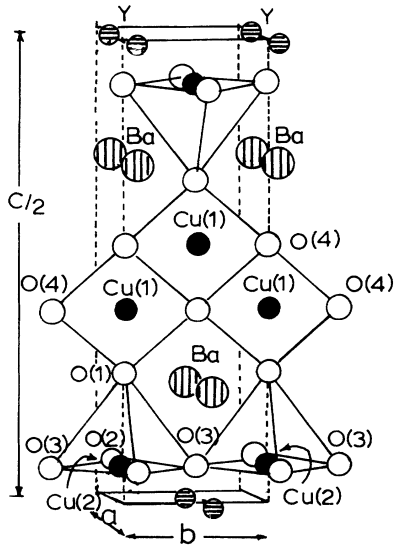

FIG. 1. Crystal structure of $YBa_2Cu_4O_8$ showing half of the unit cell. The Cu(2) sites in the planes are separated by Cu_2O_4 ribbons extending along the *b* axis.

Kaldis *et al.*[7] have recently examined the structure of 1:2:4 as a function of temperature using powder neutron-diffraction measurements. They refined their results in terms of an anisotropic MSD of atoms and have noted anomalously large displacement of the planar oxygen sites out of the planes, i.e., $\langle z^2\rangle/\langle x^2\rangle=0.62$ Å^2/0.23 Å^2=2.70 for O(2) and $\langle z^2\rangle/\langle x^2\rangle=1.03$ Å^2/0.23 Å^2=4.48 for O(3) sites. The planar Cu(2) sites also display a significant anisotropy of the MSD, with the ratio $\langle z^2\rangle/\langle x^2\rangle=1.00$ Å^2/0.15 Å=6.67. We note from their results that the Cu(2)—O(3) and Cu(2)—O(2) bond lengths of 1.95 and 1.93 Å are very nearly the same, but these are distinctly smaller than the Cu(2)—O(1) bond length with the apical oxygen atom of 2.27 Å. These bond-length results indicate that the Cu(2)—O(2) or —O(3) bond can be characterized as a "σ" bond being close to the sum of Cu^{2+} and O^{2-} covalent radii. The longer Cu(2)—O(1) bond, on the other hand, is better understood as a combination of π-σ interaction, with an attractive σ interaction resulting due to overlap of the Cu d_{z^2} and O p_z orbitals and a significant π repulsion setting in along the *z* axis between the occupied d_{xz} and d_{yz} orbitals of Cu and the p_x and p_y orbitals of the apical O(1) site. These chemical-bonding considerations permit reconciling the spatial anisotropy of the Cu(2) MSD: a smaller value (0.15 Å^2) in the plane and a much larger one (1.00 Å^2) normal to the plane. We shall return to this result later while discussing the Fe^{3+} MSD in the CuO_2 planes which displays just the reverse trend.

III. SAMPLE PREPARATION AND X-RAY DIFFRACTION

Bulk 1:2:4 superconducting samples were prepared by a solid-state reaction of $YBa_2(Cu_{1-x}Fe_x)_3O_{7-\delta}$ at $x=0$ and 0.02, and CuO precursors at 900 °C in an oxygen ambient of 221 atmospheres. Preparation of the Fe-doped 1:2:3 material has been described earlier.[8] The precursor powder mixture contained in Au tubing loosely crimped at both ends was held vertical in an autoclave and reacted for a 24-h period. Samples were then slowly cooled from 900 °C to room temperature over an 8-h period. Powder x-ray-diffraction scans of the Fe-doped 1:2:4 and pristine sample (shown in Fig. 2) display a single-phase orthorhombic sample with lattice parameters $a=3.835(2)$ Å, $b=3.870(2)$ Å, and $c=27.216(5)$ Å at $x=0$ and $a=3.835(2)$ Å, $b=3.879(2)$ Å, and $c=27.120(5)$ Å at $x=0.02$.

Some of the pristine and Fe-doped 1:2:4 polycrystalline samples were finely crushed and grain aligned at room temperature in a 9.4-T magnetic field using Duro epoxy as a potting medium. The procedure has been discussed earlier by Farrell *et al.*[3] This resulted in a pill $\sim\frac{1}{2}$ in. in diameter by $\frac{1}{16}$ in. thick with the *c* axis of the grains

along the applied magnetic field (also the pill axis). Figure 3 shows an XRD scan of the grain-aligned specimen with x rays incident on the pill face as sketched in the inset of Fig. 3. We note in Fig. 3 that only (00l) reflections are observed in this geometry. This clearly confirms the c-axis alignment of the grains perpendicular to the pill face in our samples.

The degree of grain alignment in our samples has been quantitatively checked by recording XRD scans with the x-ray beam incident perpendicular to the c axis. For this scattering geometry, only (hkl) reflections with $l=0$ are expected. We observe (110), (020), and (200) reflections as anticipated. This indicates a high degree (>98%) of grain alignment of our sample. The narrow width of the (00l) peaks seen in Fig. 3 provides further evidence that the individual grains do align with high degree of parallelism.

At low angles ($0<\theta<12°$), the XRD scans clearly show the (002), (004), and (006) reflections characteristic of the 1:2:4 phase. The c cell length of 27.2 Å in the 1:2:4 phase results in the (002) reflection at $2\theta=6.8°$ corresponding to a d spacing of 13.6 Å. The presence of the 1:2:3 and 2:4:7 phases in our samples would respectively show (001) reflections at a d spacing of 11.7 Å and (004) reflection at a d spacing of 12.55 Å from these phases. These are clearly absent in the XRD scans of our samples. Thus, XRD scans serve to confirm the single-phase nature of our samples and the high degree of grain alignment presently achieved. In some samples where the high-pressure sintering reaction did not proceed to completion either due to lack of oxygen resulting from complete crimping of both ends of the Au tubing or from a bend in the Au tubing alloying it shut at 900 °C, clear evidence of an unreacted 1:2:3 phase was observed from XRD scans. The transition temperature and Mössbauer spectra of such samples looked qualitatively different from those of the single-phase 1:2:4 samples. Results on such mixed-phase samples are excluded from this work. We suppose that one of the reasons Morris *et al.*[9] concluded a destabilization of the 1:2:4 phase occurs upon Fe doping at a concentration of only $x=0.012$ is probably the result of an incompletely oxidized precursor. In our laboratory, we have succeeded in preparing single-phase samples of Fe-doped 1:2:4 at $x=0.03$. (See Fig. 8.)

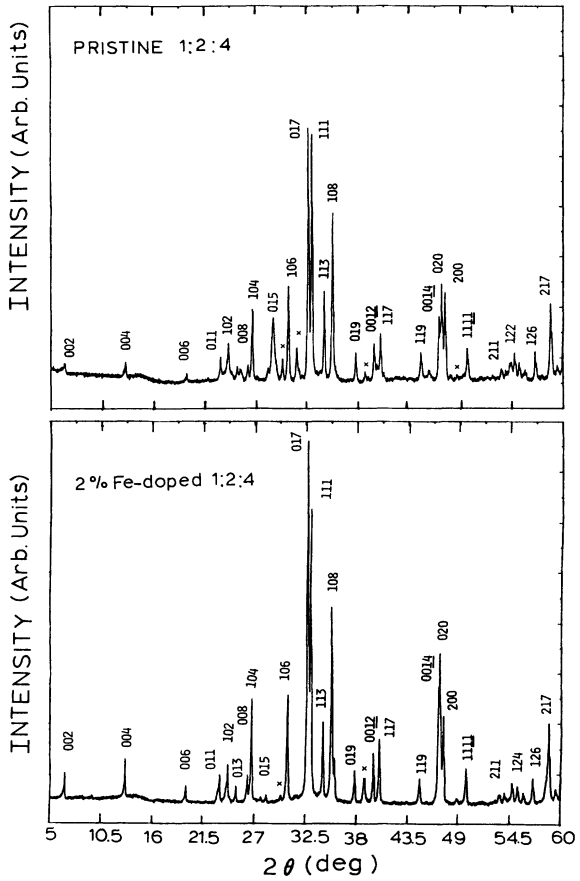

FIG. 2. XRD scans of pristine and 2 at. % Fe-doped 1:2:4 samples prepared by high-pressure sintering of precursors in an oxygen ambient reveal a remarkable similarity. The asterisks designate impurity phase peaks.

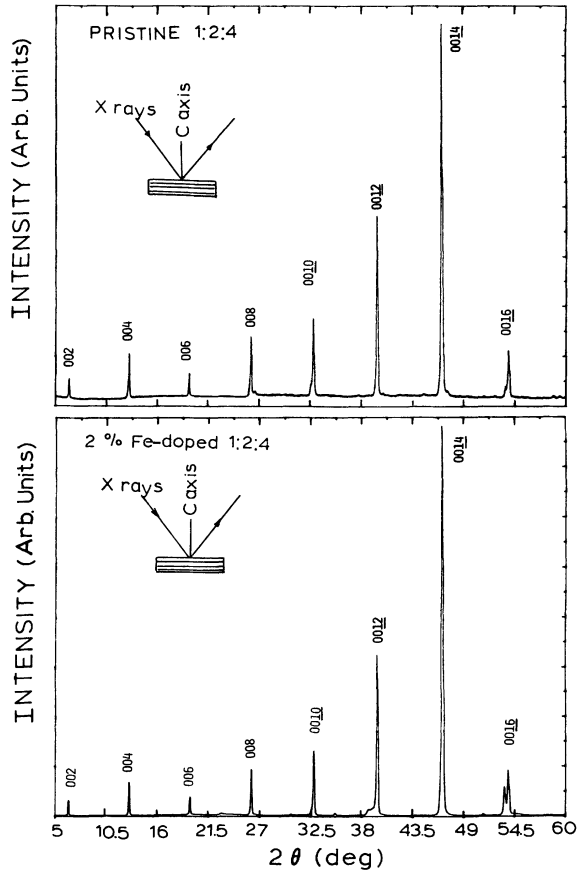

FIG. 3. XRD scans of grain-aligned pristine and 2 at. % Fe-doped 1:2:4 samples taken with x rays incident along the c axis as indicated. Only (00l) peaks are observed as expected for such a geometry confirming that the c axis of the grains align parallel to the applied external field.

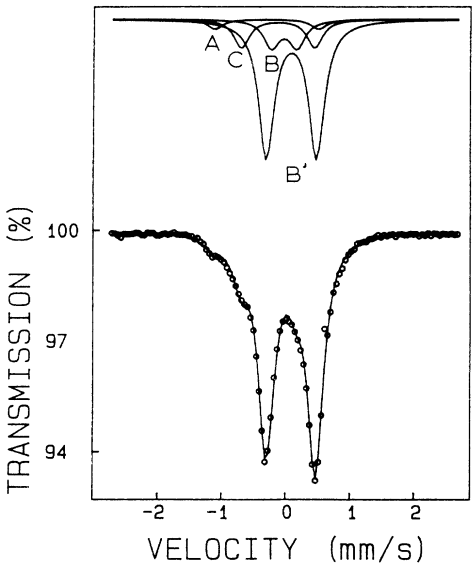

FIG. 4. Room-temperature Mössbauer-effect spectrum of a 2 at. % Fe-doped 1:2:4 sampler deconvoluted in terms of four quadrupole doublets B', B, A, and C. The former (B' and B) represent plane sites while the latter (A and C) represent defect chain sites.

IV. EXPERIMENTAL RESULTS

In this section we present Mössbauer spectroscopy and magnetization results on Fe-doped 1:2:4 samples. Results on both polycrystalline and grain-aligned specimens will be presented. In the next section we shall discuss the implications of these results.

A. Mössbauer spectroscopy

A conventional constant acceleration electromechanical drive was used to record room-temperature ^{57}Fe Mössbauer spectra using a 10 mCi ^{57}Co in Pd metal source of the 14.4-keV radiation. A Kr proportional counter was used to detect the x- and γ-ray radiation. All spectral line shapes were least-squares fit in terms of a superposition of the requisite number of doublets possessing a Lorentzian profile using software developed to run on a 286-based PC and to generate plots on a Hewlett-Packard color-pro plotter. Isomer shifts are quoted relative to α-Fe at room temperature.

Figure 4 displays spectrum of a randomly oriented 2 at. % doped 1:2:4 sample. The line shape is analyzed in terms of two majority (B',B) and two minority (A,C) quadrupole doublets with splittings and isomer shifts tabulated in Table I. The justification for line-shape analysis in terms of four sites was eluded to earlier in our work on $YBa_2(Cu_{1-x}Fe_x)_4O_8$ samples as a function of Fe concentration.[1] There we noted that sites B and B' are plane sites while the minority C and A sites represent chain sites. These latter sites are believed to occur at stacking faults in the 1:2:4 samples.

Figure 5 displays spectra of a 2 at. % Fe-doped 1:2:4 sample taken after grain alignment. Spectra taken at several tilt angles β in the range $0<\beta<\pi/2$ are

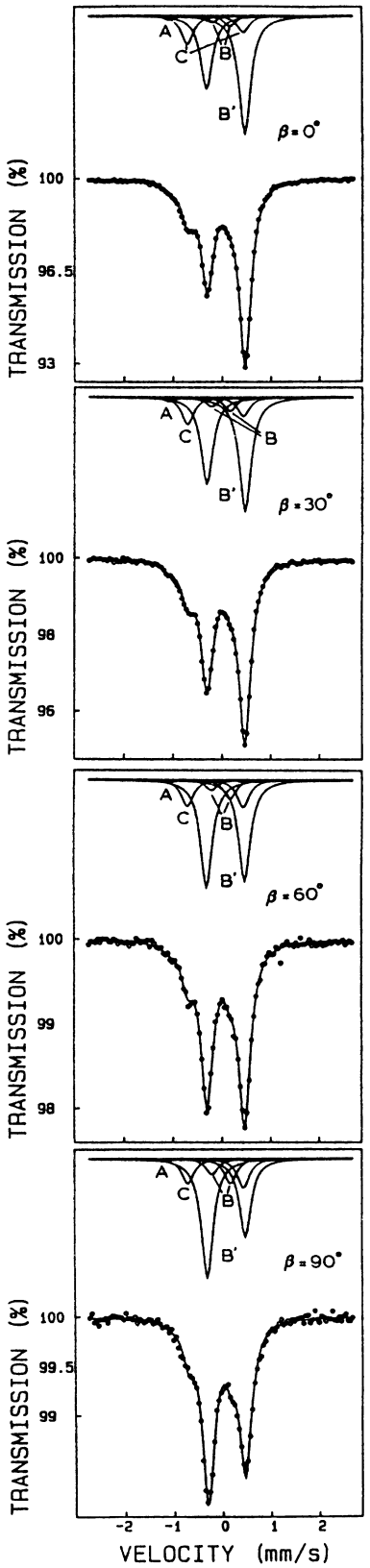

FIG. 5. Room-temperature Mössbauer-effect spectra of a 2 at. % Fe-doped 1:2:4 sample taken after grain alignment. The spectra from top to bottom are taken at tilt angles β (between **k** and the c axis as shown in inset of Fig. 6) of 0°, 30°, 60°, and 90°, respectively.

TABLE I. Room-temperature ^{57}Fe Mössbauer-effect parameters of various sites observed in the spectrum of a $YBa_2(Cu_{1-x}Fe_x)_4O_8$ $x=0.02$ sample shown in Fig. 4.

Site	δ[a] (mm/s)	Δ (mm/s)	I_n/I (%)
B'	0.31(1)	0.77(2)	0.67(3)
B	0.15(1)	0.40(5)	0.14(2)
C	0.09(1)	1.16(1)	0.14(3)
A	0.04(2)	1.84(2)	0.05(3)

[a]Relative to Fe metal at RT.

displayed. The tilt angle is defined as the angle between the c axis (also the pill axis) and the γ-ray propagation direction (see inset of Fig. 6). Note that at $\beta=0$, the positive velocity member of the B' quadrupole doublet has a larger integrated (I_+) intensity than the negative velocity member (I_-), i.e., $I_+/I_->1$. The situation is reversed at $\beta=\pi/2$ where $I_+/I_-<1$. To obtain spectra at $\beta=\pi/2$, the pill was sliced in four equal segments with a sharp knife and the pieces stacked to obtain a respectable area ($\sim\frac{1}{4}\times\frac{3}{8}$ in.^{2}) for γ propagation perpendicular to the c axis. The $I_+/I_-(\beta)$ variation for the B' doublet emerging from the spectra of Fig. 5 is summarized in Fig. 6. To deconvolute the spectra, the $I_+/I_-(\beta)$ variation for the minority A and C chain sites was kept fixed to values we observed earlier in 1:2:3 samples.[8] Furthermore, in our line-shape analysis the $I_+/I_-(\beta)$ values for the B site were constrained to those of the B' site.

We note from the spectra of Fig. 5 that the size of the Mössbauer effect along the c axis ($\beta=0$) is larger than the size perpendicular to the c axis ($\beta=\pi/2$). When the integated intensities are normalized to absorber thickness, we find that the probability of γ emission without recoil along the c axis (f_c) is larger than its value perpendicular ($f_{\perp c}$) to the c axis by a ratio of 2.0(1). The natural logarithm of the area ratio $f(\beta)/f(\pi/2)$ is plotted as a function of the angle β in Fig. 7. The smooth line is a plot of the function

$$\ln[f(\beta)/f(\pi/2)]=-k^2A_s\cos^2\beta\ ,$$

where $k=2\pi/\lambda$ is the γ-ray wave vector and $A_s=(\langle z^2\rangle-\langle x^2\rangle)$ is the MSD difference along the c axis ($\langle z^2\rangle$) and perpendicular to the c axis ($\langle x^2\rangle$). The magnitude of A_s is deduced by normalizing the observed result at $\beta=0$ and yields a value of $1.29(5)\times10^{-2}$ Å^2. The one parameter fit to the four data points in Fig. 7 does an excellent job of reproducing the results. We shall return to discuss these results in the next section.

B. Magnetization measurements

We have used a vibrating-sample-magnetometer EG and G-PAR model 4500 with an APD cryogenics Displex Helium closed-cycle cryostat (model DMX-19) to record magnetization hysteresis loops as a function of temperature in the range $11<T<300$ K. Measurements were taken on both polycrystalline and grain-aligned specimens. The former measurements permitted us to establish T_c from a T dependence of the diamagnetic susceptibility while the latter measurements made possible establishing the magnetic critical-current anisotropy in the 1:2:4 system.

Figure 8 displays the T dependence of the diamagnetic susceptibility $\chi(T)$ for the 2 at. % Fe-doped 1:2:4 sample which reveals a $T_c=62$ K. This may be compared to the T_c of a pristine 1:2:4 sample of 81.2 K. Not only does T_c decrease with x, but the width of the transition ΔT_c broadens with increasing x as well. The superconducting volume fraction of the pristine sample can be deduced from the saturation diamagnetic susceptibility $\chi_{\rm sat}$ at $T=12$ K to be 38.5×10^{-3} emu/g G. Using the theoretical density of the 1:2:4 sample as 5.889 g/cm^3, we obtain a dimensionless $\chi=25.2\times10^{-3}$ which represents about 24% of $1/4\pi$. The plot of Fig. 8 shows that substantial

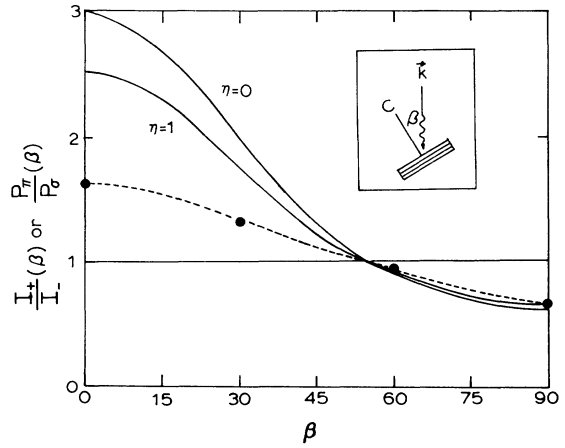

FIG. 6. Measured quadrupolar doublet intensity ratio $I_+/I_-(\beta)$ as a function of β deduced from spectra of Fig. 5 is plotted as data points and joined by a dashed line as a guide to the eye. $P_\pi/P_\sigma(\beta)$ as a function of β for $\eta=0$ and $\eta=1$ shown as continuous lines are plots of Eq. (5) in text.

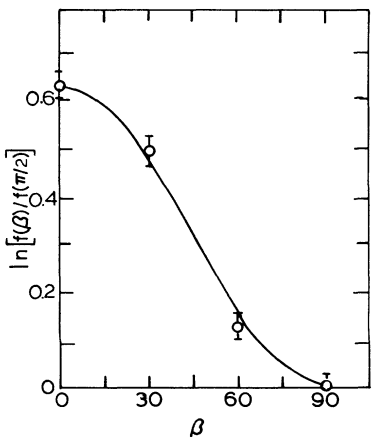

FIG. 7. Natural logarithm of the f factor normalized to its value at $\beta=\pi/2$, $\ln f(\beta)/f(\pi/2)$ as a function of β deduced from the spectra of Fig. 5. The solid line is a plot of Eq. (3) with the ratio normalized at $\beta=0$.

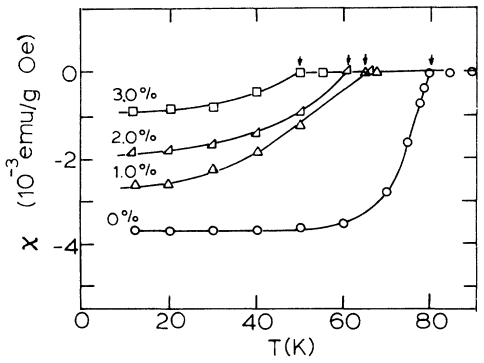

FIG. 8. dc susceptibility $\chi(x,T)$ of Fe-doped 1:2:4 samples deduced from vibrating sample magnetometry. The Fe-doping concentrations, x, are indicated in %.

reduction in the superconducting volume fraction occurs in proportion to Fe doping in 1:2:4 samples.

A grain-aligned sample mounted on a VSM sample holder was inserted in the sample chamber so that the c axis was nominally parallel to the external magnetic field from a 10-kOe electromagnet. Next, the head of the VSM was rotated by angle θ in relation to the magnetic-field axis, and the magnetization response recorded as a function of θ. A maximum in the magnetization signal was chosen to define $\theta=0$, i.e., the sample c axis parallel to H.

Figure 9 displays the magnetization hysteresis loops for the pristine sample taken for H parallel and perpendicular to the c axis. We note that the magnetization hysteresis Δm at an external field $H=5$ kOe in the parallel geometry exceeds the one in the perpendicular geometry by a ratio $\Delta m_c/\Delta m_{\perp c}=3.25$. This ratio was found not to change measurably in the Fe-doped 1:2:4 samples. We shall return to discuss the underlying critical current anisotropy in Sec. V.

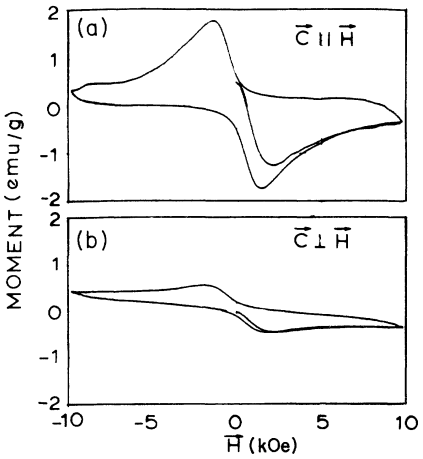

FIG. 9. Magnetization hysteresis loops for grain-aligned pristine 1:2:4 samples taken with the c axis parallel (a) and perpendicular (b) to the applied magnetic field H. The larger loop in the top panel shows that J_c flowing in the CuO_2 planes is larger than $J_{\perp c}$ normal to the planes by a factor of 3.25.

V. DISCUSSION OF RESULTS

From a compositional study of the $YBa_2(Cu_{1-x}Fe_x)_4O_8$ system, the microscopic nature of the Fe-dopant planar sites (B and B') in the 1:2:4 host was elucidated in Ref. 1. It may be pertinent to recall here that site B' is thought to represent Fe^{3+} replacing Cu(2) sites and to possess a square pyramidal coordination, similar though not identical to the Cu(2) cation. Site B is a variant of site B' and is thought to possess a quasioctahedral coordination. Such a coordination is realized with occupancy of the oxygen vacancy site in the Y plane in the immediate vicinity of site B'.

Site B may thus be visualized as the fate of site B' when oxygen is locally absorbed in the Fe-doped 1:2:4 material. The results presented in this work permit us to establish the MSD and EFG tensors for the planar site B'. In addition to these two results, we shall also discuss the critical-current anisotropy deduced presently from grain-aligned 1:2:4 samples in the following section.

A. ^{57}Fe mean-square-displacement tensor in CuO_2 planes

An upper limit to the effective absorber thickness $T=n\sigma_0 f$ of the 2 at. % Fe-doped 1:2:4 sample used in our Mössbauer measurements is calculated from the mass per unit area of the absorber, and it is found to be $T=0.45(5)$, taking $f=1$. This represents a thin absorber by definition. The integrated area under the resonance in such a case becomes directly proportional to the f factor.

If Fe were to substitute at Cu(2) sites in the host structure, given the cylindrical symmetry of this site, one expects the angular dependence of the f factor to be given by

$$f(\beta)=\exp(-k^2\langle z^2\rangle\cos^2\beta-k^2\langle x^2\rangle\sin^2\beta)\ , \tag{1}$$

where $\langle z^2\rangle$ and $\langle x^2\rangle$ represents the MSD perpendicular and parallel to the CuO_2 planes and β the polar angle with respect to the c axis. Equation (1) can be rewritten as follows:

$$f(\beta)=e^{-k^2A_s\cos^2\beta}e^{-k^2\langle x^2\rangle}\ , \tag{2}$$

where $A_s=\langle z^2\rangle-\langle x^2\rangle$ and is a measure of the asymmetry in the MSD. Equation (2) implies that

$$\ln\frac{f(\beta)}{f(\pi/2)}=-k^2A_s\cos^2\beta\ . \tag{3}$$

Equation (3) provides a justification for the plot of Fig. 7 which yielded $A_s=1.29(5)\times10^{-2}$ Å^2 or

$$f(0)/f(\pi/2)=f_c/f_{\perp c}=2.0(1)\ .$$

We have independently measured the T dependence of the f factor of site B' in grain-aligned samples for **k** parallel to the c axis and find that the $f(T)$ results are consistent with a Debye temperature $\theta_D=450(10)$ K. This leads to an f factor along the c axis at room temperature of

$$f_c=0.81(3)\ .$$

Given that $f_c/f_{\perp c}=2.(1)$, it follows that $f_{\perp c}=0.40$. At room temperature we thus obtain, for the Fe dopant,

$$\langle z^2\rangle_{\mathrm{Fe}}=0.39\times10^{-2}\ \text{Å}^2\ ,$$
$$\langle x^2\rangle_{\mathrm{Fe}}=1.68\times10^{-2}\ \text{Å}^2\ .$$

Thus, the Fe MSD parallel to the CuO_2 plane ($\langle x^2\rangle_{\mathrm{Fe}}$) is a factor of 4.27 larger than the displacement perpendicular to the planes ($\langle z^2\rangle_{\mathrm{Fe}}$). Powder neutron-diffraction measurements[7] reveal that the MSD of Cu(2) sites in this material are

$$\langle z^2\rangle_{\mathrm{Cu}}=1.31\times10^{-2}\ \text{Å}^2\ ,$$
$$\langle x^2\rangle_{\mathrm{Cu}}=0.26\times10^{-2}\ \text{Å}^2\ ,$$

i.e., the displacement of Cu(2) sites parallel to the planes ($\langle x^2\rangle_{\mathrm{Cu}}$) is nearly a factor of 5 smaller than its magnitude perpendicular to the planes ($\langle z^2\rangle_{\mathrm{Cu}}$). Given that Cu(2)—O(2) and Cu(2)—O(3) bond lengths of 1.93 and 1.95 Å in the plane are significantly shorter than the Cu(2)—O(1) bond length of 2.28 Å perpendicular to the planes, the smaller MSD of Cu(2) in the plane can be reconciled more or less.

To reconcile the ^{57}Fe MSD results with site location in the planes, we must require the dopant to be displaced away from the planes along the c axis to form a σ bond of about 1.90 Å with the apical O(1) sites as shown in Fig. 10. The Fe bond length with the O(2) and O(3) sites in the planes, as a consequence of the displacement towards the O(1) site, is probably increased to 2.0 Å in relation to that of Cu of 1.94 Å, but must clearly continue to be primarily σ in character involving Fe $d_{x^2-y^2}$ state overlapping with O p_x and p_y states.

The shorter length of the Fe^{3+}—O(1) bond (1.90 Å) in relation to the Cu^{2+}—O(1) bond (2.28 Å) suggested above could originate chemically from a reduced π repulsion between the d_{xz}, d_{yz}, and p_x and p_y orbitals. We note that, for Cu^{2+}, the d_{xy} orbital is fully occupied while for Fe^{3+} only half occupied as illustrated in Fig. 11. Furthermore, the higher cation charge for Fe^{3+} in relation to Cu^{2+} will result in a larger Coulomb repulsion from the Y^{3+} plane, thus again forcing the dopant to be displaced away from the CuO_2 planes towards the apical O(1) oxygen site. Finally, the ionic radius of Fe^{3+} (0.55 Å) is smaller than that of Cu^{2+} (0.62 Å) leading to a smaller σ bond length of Fe^{3+}—O(1) in relation to the Cu^{2+}—O(1) bond.

It is pertinent to remark here that the B' site isomer shift is characteristic of a high-spin Fe^{3+} species and the relevant crystal-field splittings are illustrated in Fig. 11. For a high-spin Fe^{3+} species ($S_z=\frac{5}{2}$), one predicts an internal magnetic field (H_{hf}) of about 55 T following the $22\langle S_z\rangle$ rule. Indeed, we have observed magnetic ordering at low T ($T=4.2$ K) revealing $H_{hf}\sim44.6(3)$ T for site B', confirming the proposed spin assignment from the isomer shift. This is a point we shall elaborate in a forthcoming publication where T-dependent Mössbauer spectroscopy results will be discussed on the present system comprehensively.

The spatial anisotropy of the MSD associated with the B' site is unusual. To gain insights into this result, it is instructive to compare the present result to the celebrated case of a CsC_8 graphite-intercalation compound. Large anisotropies in the f factor were documented earlier[10] for CsC_8 using the ^{133}Cs Mössbauer effect. In graphite, the in-plane versus out-of-plane chemical bonding is, of course, known to be strikingly different, being covalent in one case and van der Waals in the other. In spite of this we note that the observed f-factor anisotropy $f_{\perp c}/f_c=20$ for CsC_8 translates into a MSD ratio $\langle z^2\rangle/\langle x^2\rangle$ of only $\frac{1}{2}$. The higher energy of the γ transition in ^{133}Cs (81 keV) versus ^{57}Fe (14.4 keV) makes f factors in Cs very sensitive to small changes in the MSD. The Fe dopant in the planes of the 1:2:4 material clearly

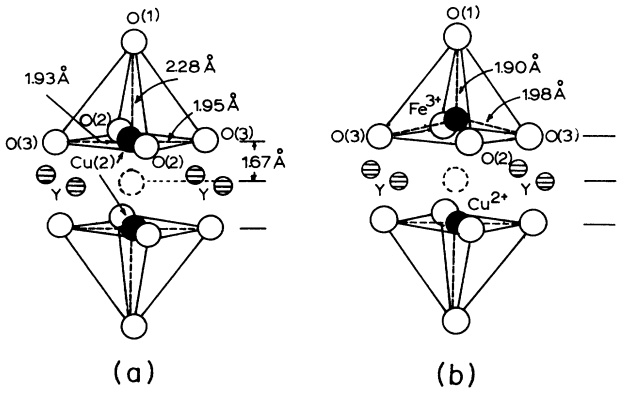

FIG. 10. (a) The coordination of Cu(2) sites in pristine 1:2:4 showing the square pyramidal geometry, (b) the proposed coordination of site B' showing Fe localized in the planes as suggested from the Mössbauer spectroscopy measurements. Note that, when the vacant oxygen site in the Y-plane is occupied in the vicinity of the Fe dopant, the quasioctahedral site in question becomes site B.

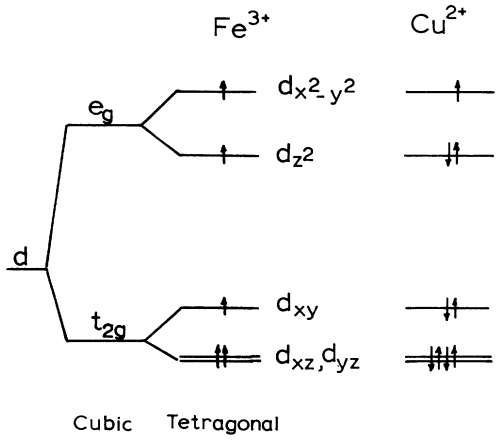

FIG. 11. Crystal-field levels of Fe^{3+} high spin (site B') and Cu^{2+} in a cubic and tetragonal field.

displays a larger anisotropy of the MSD than even Cs in CsC_8. Such an extraordinary result, in our view, cannot be reconciled in terms of purely harmonic interatomic forces, particularly because one does not expect Fe in-plane and out-of-plane chemical bonding in the CuO_2 planes to be all that different in character. It is clear from these room-temperature MSD results that the motion of Fe parallel to the CuO_2 plane is rather unusual and is a point we shall return to in our discussion of the EFG tensor next.

B. ^{57}Fe electric-field-gradient tensor in CuO_2 planes

The sign of the quadrupole coupling e^2qQ is uniquely fixed if one can identify the positive velocity peak in a Mössbauer spectrum with either the $\pi(\frac{3}{2}\rightarrow\frac{1}{2})$ or $\sigma(\frac{1}{2}\rightarrow\frac{1}{2})$ quadrupole component. It is well known that the angular distribution of the π and σ quadrupole components in the principal axis system (PAS) of the EFG tensor is given[11] by

$$P_{\pi(\sigma)}(\theta\phi) = \frac{1}{2}+(-)\frac{1}{8(1+\eta^2/3)^{1/2}}(3\cos^2\theta-1+\eta\sin^2\theta\cos^2\phi)\ , \tag{4}$$

where $\eta=(V_{xx}-V_{yy})/V_{zz}$ and θ,ϕ represent γ-ray propagation direction relative to the PAS system of the EFG tensor.

In a previous paper,[11] we examined the consequences of two obvious possibilities for the orientation of PAS of the EFG tensor with respect to the crystal axes in orthorhombic $YBa_2Cu_3O_{7-\delta}$; one when V_{zz} is parallel to the c axis and the other when it is perpendicular to it. We noted that, in the former case, $\theta=\beta$, and the angular distributions simplify to

$$P_{\pi(\sigma)}(\beta)=\frac{1}{2}+(-)\frac{3\cos^2\beta-1}{8(1+\eta^2/3)^{1/2}}\ . \tag{5}$$

If Fe substitutes at Cu(2) sites in the orthorhombic 1:2:4 structure, the local site symmetry requires V_{zz} at Fe, as at Cu(2) sites, to reside along the c axis. Furthermore, since Cu(2)—O(2) and Cu(2)—O(3) bond lengths in the pristine material are nearly the same, one can expect the ^{57}Fe EFG tensor to be axially symmetric ($\eta\simeq0$), as deduced by Brinkmann[12] and several other groups from ^{63}Cu and ^{65}Cu NQR studies on the pristine material. If the Fe dopant does not substitute Cu(2) sites but is displaced towards the apical oxygen site O(1) along the Cu(2)—O(1) bond axis, one still expects V_{zz} to continue to reside along the c axis and the asymmetry parameter $\eta\sim0$. The expected theoretical variation of the intensity ratio $P_\pi/P_\sigma(\beta)$ for the two extreme η values is plotted in Fig. 6 as the solid curves. While these theoretical curves broadly reproduce the overall trend of the present experimental results (shown by the solid circles and dashed line), it is nevertheless also clear that there is a substantial discrepancy by nearly a factor of 2 between the observed ($I_+/I_-=1.7$) and the expected ($P_\pi/P_\sigma=3.0$) quadrupolar doublet intensity asymmetry at $\beta=0$. It would be pertinent to remark here that $I_+/I_-(\beta)$ trends for the chain sites A and C that we examined earlier[11] in grain-aligned 1:2:3 samples display two features that are distinct from the ones observed in the plane sites B and B'. First, the $I_+/I_-(\beta)$ variation for the chain sites displays a pattern that has the opposite sense than the one seen for the plane sites. Second, the measured $I_+/I_-(\beta)$ ratio for the chain sites agrees remarkably well with the expected $P_\pi/P_\sigma(\beta)$ ratio in the static case.

One can categorically state that, if one identifies the positive (negative) velocity components of the site B' quadrupole doublet with the π (σ) transitions, then the sign of the quadrupole coupling (e^2qQ) is positive, i.e., the sign of V_{zz} is positive, as the sign of the ^{57}Fe nuclear quadrupole moment (Q) is known[13] to be positive (+0.082) b. A point-charge calculation of the EFG due to the five nearest-neighbor (NN) oxygen sites yields a positive sign for V_{zz} as expected from local site-symmetry considerations. Such a solution appears to us to be the physically plausible one because of the absence of the sixth-NN oxygen site in the Y plane. Such a coordination will give rise to a prolate charge (positive) distribution around the Fe^{3+} cation.

We next consider the reverse assignment, i.e., the positive (negative) quadrupole component represent the σ (π) transition. Only for V_{zz} directed perpendicular to the c axis can one expect the $P_\sigma/P_\pi(\beta)$ trend to match up with observed behavior of $I_+/I_-(\beta)$. This assignment leads at $\beta=0$, $P_\sigma/P_\pi=5/3\simeq1.7$, which fits the observed $I_+/I_-(\beta=0)$ of 1.7 perfectly. At $\beta=\pi/2$, we recognize that a spatial averaging occurs since the a and b axes occur randomly in the plane normal to the c axis in these grain-aligned specimens. Theoretically, one expects the ratio $P_\sigma/P_\pi(\beta=\pi/2)=0.78$, which may be compared to the observed $I_+/I_-(\beta=\pi/2)=0.62(2)$. Here, again, we note a significant discrepancy between the observed and expected intensity ratio. The present assignment leads to a negative V_{zz}, however. This, in our judgment, is physically implausible for a planar site given the square pyramidal coordination of site B'. It is on this basis we reject the assignment of a negative quadrupole coupling for site B'.

For a positive e^2qQ, the discrepancy between $I_+/I_-(\beta=0)=1.7$ and the expected $P_\pi/P_\sigma(\beta=0)=3.0$ has a trivial explanation, viz., the grain-aligned samples are only partially aligned. To account for a reduction in the $I_+/I_-(\beta=0)$ ratio by a factor of 2 would require the grains to be misaligned relative to the c axis by at least 35° on an average. This may be seen from Fig. 6 where the $P_\pi/P_\sigma(\beta)$ plot at $\eta=0$ shows a halving from $\beta=0$ to $\beta=35°$. Such an explanation appears untenable to us given the high degree (>98%) of grain alignment suggested by our XRD scans and the narrow width of the Bragg peaks.

A physically more plausible reason for the factor of 2 loss in the quadrupole intensity asymmetry $I_+/I_-(\beta=0)$ probably results from an averaging process intrinsic to the layered structure of these cuprates, i.e., a stationary fluctuation of the EFG in the planes. Specifically, we propose that a motion of the planar oxygen O(3) and O(2) sites normal to the planes produces a time-dependent

EFG. In the cuprates the large displacements inferred from static structure factors (neutron-diffraction measurements[7]) may indicate possible dynamical effects, with anions and cations hopping between two locations in an anharmonic (flat-bottomed or double-well) potential. Consider, for example, the out-of-phase displacement of the planar oxygen sites O(3) and O(2) normal to the planes as sketched in Fig. 12. The mode in question is not Raman active.[14] We visualize the rocking motion of the planar oxygen sites to produce a fluctuating EFG at the Fe-dopant site. Given that the O(3) oxygen sites displace as much as 0.11 Å normal to the planes, we can expect not only (i) the magnitude of V_{zz} to change as the FeO_5 polyhedron rocks, but also (ii) the direction of V_{zz} to tilt relative to the c axis. Furthermore, if the displacements of the O(2) and O(3) oxygen atoms normal to the planes are unequal, as is suggested by the powder neutron-diffraction measurements,[7] then the square base of the FeO_5 polyhedron in its mean position will undergo a rhombic distortion at the extreme positions. Such a (iii) dynamic change in symmetry will induce a finite η for the EFG tensor. Thus, we believe factors (i), (ii), and (iii) associated with the rocking vibration of the planar oxygen sites, each additively contribute to a motional averaging of the quadrupolar doublet intensity ratio (I_+/I_-) and lowers the observed value (1.7) in relation to the theoretically expected value (3.0) for a static EFG. Here we believe that the correlation time for the fluctuation (τ_c) is much smaller than the interaction time ($\tau_{\rm int}$) for the ^{57}Fe nucleus to sense the EFG. From the observed quadrupole splitting, we calculate $\tau_{\rm int}=\hbar/\Delta Eq=8.8$ ns and believe that τ_c indeed must be $\ll\tau_{\rm int}$, since τ_c determined by Debye frequencies is of the order of 10^{-12} s. This insures stationary relaxation in the fast-relaxation regime at room temperature. A detailed theoretical calculation of a fluctuating EFG based on such a model is certainly in order to check the validity of these ideas.

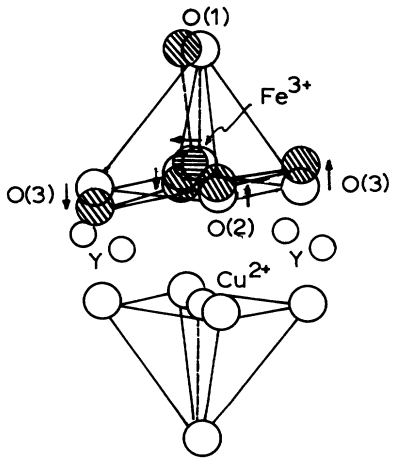

FIG. 12. Fluctuating EFG at Fe^{3+} (site B') induced by an out-of-phase motion of planar oxygen sites O(3) and O(2) normal to the planes. This vibrational mode motionally averages the asymmetry (I_+/I_-) of the quadrupole doublet. Note that the proposed vibrational mode also induces motion of the Fe^{3+} cation parallel to the CuO_2 planes.

An attractive feature of the mode vibration sketched in Fig. 12 is its affect on the vibrational motion of the Fe^{3+} cation. In relation to the Cu(2) sites, we noted earlier that the Fe-dopant site is displaced away from the planes by about 0.4 Å. One expects the Fe dopant to respond to the planar oxygen site motion normal to the planes by executing displacements parallel to the planes. We will present experimental evidence to suggest that the Fe motion parallel to the planes is rather anharmonic.[15] The root-mean-square amplitude of Fe motion parallel to the planes, i.e., $\sqrt{\langle x^2\rangle}=0.13$ Å, and it amounts to 6% of the Fe—O(2) and Fe—O(3) bond length. It is difficult to understand as large a spatial anisotropy of the MSD as we have observed for Fe in the planes if one assumes that the Fe bonding with its five oxygen NN's (all bond lengths 1.9–2.0 Å to be described by harmonic forces alone).

C. Critical-current anisotropy in 1:2:4

One may use the Bean critical state model to extract the critical current (J_c) from a measurement of the magnetization hysterisis Δm for a superconducting sample containing grains of radius r using the relation

$$J_c(\mathrm{A/cm^2})=\frac{17\Delta(\mathrm{emu/cm^3})}{r(\mathrm{cm})} . \tag{6}$$

Since the observed magnetization hysterisis Δm parallel and normal to the c axis differ by a factor of 3.25, we conclude that

$$J_{\perp c}/J_{\parallel c}=3.25 .$$

The absolute value of J_c at $H=5$ kOe is calculated from the Bean formula using $r=5$ μm, $\Delta m=1$ emu/g, and a theoretical density of 5.89 g/cm^3 to be $J_c=2\times10^6$ A/cm^2 at 12 K. This may be compared to a value of $J_c=2\times10^7$ A/cm^2 in 1:2:3 material at 4.25 K. Although the absolute value of J_c decreases slightly upon Fe doping, the critical-current anisotropy $J_c/J_{\perp c}$ remains largely insensitive to Fe-doping concentrations in the range ($x\lesssim0.02$). Given that the Fe dopant in the 1:2:4 samples is known to localize in the CuO_2 planes, it is clear that such doping does not enhance flux pinning yielding a higher J_c.

A somewhat higher critical-current anisotropy , $J_c/J_{\perp c}$ of ~10, is documented for the Y-based 1:2:3 material.[3] The insertion of an additional chain in the 1:2:3 structure, to realize the 1:2:4 structure, may lower the critical-current anisotropy largely because of an increase in $J_{\perp c}$. The "ribbons" in the 1:2:4 phase provide additional supercurrent paths transverse to the planes when a magnetic field is applied parallel to the planes.

Critical currents and flux pinning at microstructural defects in oxide superconductors is a rapidly evolving area.[16] In spite of the short coherence length of 5–20 Å, the present results show that point defects like Fe dopants in the planes are too small to act as flux-pinning centers. Larger entities such as stacking faults in mixed-phase (1:2:3 and 2:4:7) materials and twin planes in 1:2:3 material apparently do indeed enhance J_c by acting as flux-pinning centers.

VI. CONCLUSIONS

In summary, the use of grain-aligned $YBa_2(Cu_{1-x}Fe_x)_4O_8$ samples in Mössbauer and magnetization experiments has permitted us to establish (a) the spatial anisotropy of the MSD, (b) the orientation of the EFG tensor for the Fe^{3+} dopant site localized in the planes, and (c) the critical-current anisotropy $J_c/J_{\perp c}$ in 1:2:4 material and its dependence on Fe doping. Our results show that the Fe MSD parallel and perpendicular to the CuO_2 exhibits a ratio $\langle x^2\rangle/\langle z^2\rangle = 4.27(10)$ which is in sharp contrast to the corresponding anisotropy for the Cu^{2+} cation of 0.22 recently measured from powder neutron-diffraction experiments.[7] It is suggested that, when Fe substitutes Cu(2) sites, Fe is localized away from the planes towards the apical O(1) sites and probably moves in an anharmonic potential parallel to the planes to account for the substantial anisotrophy of the MSD. The ^{57}Fe EFG in the planes is consistent with a positive sign with V_{zz} directed along the c axis but fluctuating rapidly at 300 K to motionally average the quadrupolar doublet intensity asymmetry observed along the c axis. The fluctuations are thought to derive from a rocking motion of the FeO_5 polyhedra as the planar oxygen sites O(3) and O(2) display an out-of-phase vibrational motion normal to the planes. The critical-current anisotropy established from dc magnetization measurements using a VSM show that $J_c/J_{\perp c} = 3.25$ at 12 K and is insensitive to Fe doping in the planes at low doping concentrations ($0 < x < 0.02$). The critical-current anisotropy in the 1:2:4 material reported here is a factor of 3 smaller than the one found in the corresponding 1:2:3 material. This suggests that the presence of the chemically more stable ribbons in the former material provides current paths normal to the planes and enhances $J_{\perp c}$ in relation to the currents flowing in the linear chains of the 1:2:3 material.

ACKNOWLEDGMENTS

We are particularly grateful to Professor A Kilinc for making available facilities in his high-pressure laboratory to synthesize the 1:2:4 material. This work was supported by NSF Grant No. DMR-89-02836 at University of Cincinnati and NSF Grant No. DMR 89-13651 at Case Western Reserve University. We particularly appreciate partial support from the University of Cincinnati.

[1] S. Pradhan, P. Boolchand, Y. Wu, D. McDaniel, A. Kilinc, and W. Huff (unpublished).

[2] See, for example, P. Boolchand and D. McDaniel, in *Studies on High-Temperature Superconductors,* edited by Anant V. Narlikar (Nova Science, New York, 1990), Vol. 4, p. 143. This review article references work of numerous groups that have examined the Fe-doped 1:2:3 system using Mössbauer spectroscopy.

[3] D. E. Farrell, B. S. Chandrasekhar, M. R. DeGuire, M. M. Fang, V. G. Kogan, J. R. Clem, and D. K. Finnemore, Phys. Rev. B **36**, 4025 (1987).

[4] P. Fischer, J. Karpinski, E. Kaldis, E. Jilek, and S. Rusiecki, Solid State Commun. **69**, 531 (1989).

[5] R. M. Hazen, L. W. Finger, and D. E. Morris, Appl. Phys. Lett. **54**, 1057 (1989).

[6] Donald E. Morris, Janice H. Nickel, John Y. T. Wei, Naggi G. Asmar, Jeffrey S. Scott, Ulrich M. Scheven, Charles T. Hultgren, Andrea G. Markelz, Jeffrey E. Post, Peter J. Heaney, David R. Veblen, and Robert M. Hazen, Phys. Rev. B **39**, 7347 (1989).

[7] E. Kaldis, P. Fischer, A. W. Hewat, E. A. Hewat, J. Karpinski, and S. Rusiecki, Physica C **159**, 668 (1989).

[8] C. Blue, K. Elgaid, I. Zitkovsky, P. Boolchand, D. McDaniel, W. C. H. Joiner, J. Oostens, and W. Huff, Phys. Rev. B **37**, 5905 (1988).

[9] D. E. Morris, A. P. Marathe, and A. P. B. Sinha, Physica C **169**, 386 (1990).

[10] L. E. Campbell, G. L. Montet, and G. J. Perlow, Phys. Rev. B **15**, 3318 (1977).

[11] P. Boolchand, C. Blue, K. Elgaid, I. Zitkovsky, D. McDaniel, W. Huff, B. Goodman, G. Lemon, D. E. Farrell, and B. S. Chandrasekhar, Phys. Rev. B **38**, 11 313 (1988). Also see F. Hartmann-Boutron and Y. Gros, Physica C **172**, 287 (1990).

[12] D. Brinkmann, Z. Naturforsch Teil A **44**, 1 (1989); also see, H. Zimmermann *et al.*, Physica C **159**, 681 (1989).

[13] R. J. Duff, Phys. Rev. Lett. **25**, 1611 (1981).

[14] C. Thomson, M. Cardona, W. Kress, R. Liu, L. Genzel, M. Bauer, L. Schonherr, and W. Schröder, Solid State Commun. **65**, 1139 (1988).

[15] ^{57}Fe Mössbauer Debye-Waller Factor $f(T)$ measurements on grain-aligned 1:2:4 samples parallel to CuO_2 display the lack of any T dependence in the range $11 < T < 300$ K. This is suggestive of anharmonic behavior and is planned to be discussed in a forthcoming publication.

[16] See, for example, Cryogenics **30** (1990), May issue, which has several articles on cirtical currents and flux pinning in high-T_c superconductors.